Water Science & Technology

Water Science & Technology Vol 89 No 8, 2118 doi: 10.2166/wst.2024.120

Coupling of biogas residue biochar and low-magnitude electric fields promotes anaerobic co-digestion of sewage sludge and food waste

Hongbo Liu[a], Peng He[a], Yang Chen[a], Xingkang Wang[a], Ruixiang Zou[a], Tao Xing[b,c], Suyun Xu[a], Chengyang Wu[a,*], Claudia Maurer[d] and Eric Lichtfouse[e]

[a] School of Environment and Architecture, University of Shanghai for Science and Technology, 516 Jungong Road, Shanghai, China
[b] Jiangsu Lianxing Complete Equipment Manufacturing Co., Ltd, 96 Feiyue Road, Jingjiang, Jiangsu, China
[c] Jiangsu Dingxin Environmental Protection Technology Co., Ltd, 95 Feiyue Road, Jingjiang, Jiangsu, China
[d] University of Stuttgart – Institute of Sanitary Engineering, Water Quality and 12 Waste Management, Bandtäle 2, Stuttgart 70569, Germany
[e] State Key Laboratory of Multiphase Flow in Power Engineering, Xi'an Jiaotong University, 28 Xianning West Rd, Xi'an, Shaanxi 710049, China
*Corresponding author. E-mail: wcy@usst.edu.cn

HL, 0000-0002-2672-7262

ABSTRACT

Biochar-assisted anaerobic digestion (AD) remains constrained due to the inefficient decomposition of complex organics, even with the direct interspecies electron transfer (DIET) pathway. The coupling of electrochemistry with the anaerobic biological treatment could shorten lengthy retention time in co-digestion by improving electron transfer rates and inducing functional microbial acclimation. Thus, this work investigated the potential of improving the performance of AD by coupling low-magnitude electric fields with biochar derived from the anaerobically digested biogas residue. Different voltages (0.3, 0.6, and 0.9 V) were applied at various stages to assess the impact on biochar-assisted AD. The results indicate that an external voltage of 0.3 V, coupled with 5 g/L of biochar, elevates CH_4 yield by 45.5% compared to biogas residue biochar alone, and the coupled approach increased biogas production by up to 143% within 10 days. This finding may be partly explained by the enhanced utilization of substrates and the increased amounts of specific methanogens such as *Methanobacterium* and *Methanosarcina*. The abundance of the former increased from 4.0 to 11.3%, which enhances the DIET between microorganisms. Furthermore, the coupling method shows better potential for enhancing AD compared to preparing iron-based biochar, and these results present potential avenues for its broader applications.

Key words: accelerated start-up, biogas residue biochar, co-digestion, electric field, improved methane quality, increased methane production

HIGHLIGHTS

- Biochar coupled with electric fields was used to enhance AD.
- Coupling of biogas residue biochar and electric fields accelerated the initiation of AD.
- The coupled approach improved biogas production by 143% within 10 days.
- The abundance of DIET-mediated *Methanobacterium* was improved to 11.27%.

GRAPHICAL ABSTRACT

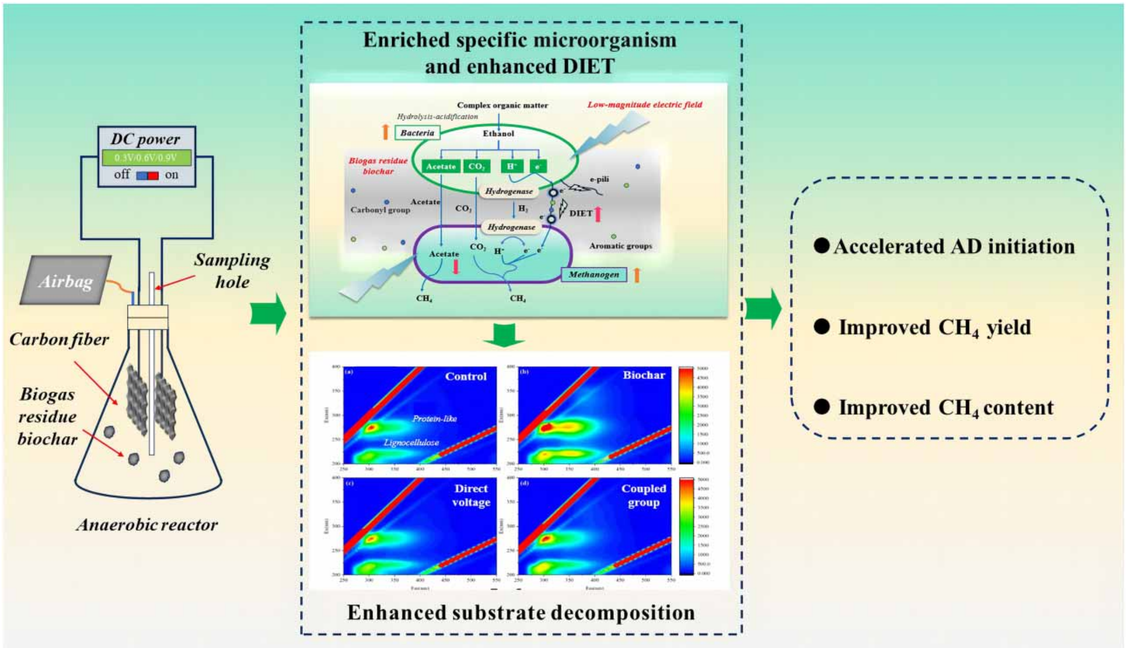

1. INTRODUCTION

Sewage sludge and food waste are significant components of municipal solid wastes generated in large quantities worldwide due to rapid urbanization and population growth (Zhang *et al.* 2023; Thakur *et al.* 2024). The proper management of these abundant waste streams is imperative because of their significant organic matter content, which is widely recognized as a potential renewable energy source (Zhang *et al.* 2023; Zhu *et al.* 2023). Anaerobic digestion (AD) could convert these organic wastes into clean energy, specifically methane (CH_4), which facilitates resource recycling and reduces carbon emissions from waste management (Hao *et al.* 2015). Unsatisfactory methane production efficiency and a lengthy retention time hinder widespread applications of AD (Liang *et al.* 2021; Jin *et al.* 2023). The disposal of huge amounts of biogas residues as an unwanted by-product poses an additional hurdle (Fuchs & Drosg 2013). Thus, it is essential to explore efficient and economical strategies to enhance AD and facilitate the disposal of by-products.

The addition of biochar has emerged as an economic and eco-friendly strategy to enhance the performance of AD, which boasts wide raw material compatibility and low production costs (Jin *et al.* 2023; Xu *et al.* 2023). The porous surface of biochar provides an ideal substrate for microorganisms to attach. This increases the digestibility of substrates and accelerates the start-up for digestion (Wu *et al.* 2022). Its unique structure could enhance pH buffering, avoid ammonia inhibition, and improve the stability and methane production of the AD process (Hoang *et al.* 2022). Biochar made from biogas residues has the potential to improve the efficiency of direct interspecies electron transfer (DIET) and enhance AD (Liu *et al.* 2022b). However, enhanced AD through the DIET mediated by conductive materials is limited due to high substrate selectivity and difficult decomposition of some substrates (Liu *et al.* 2022a; Jin *et al.* 2023).

Electrochemistry combined with anaerobic biological treatment could shorten stabilization time and improve the methane yield of AD (Park *et al.* 2019; Mendoza-Tinoco *et al.* 2023). Low-magnitude electric fields boost electron transfer efficiency and activating microorganisms, enhancing organic removal and methane production (Mendoza-Tinoco *et al.* 2023). For example, applying an external voltage of 0.1 V could promote DIET efficiency during the AD of synthetic brewery wastewater. This could result in a 23.4% higher cumulative methane yield and a 16.7% improvement in COD removal efficiency (Sun *et al.* 2020). An external voltage of 0.7 V could increase the communities of *Geobacter* and *Methanosarcina* in AD, promoting the efficiency of the DIET in the system (Gao *et al.* 2017). Thus, combining low-magnitude electric fields with biochar holds promise to overcome the limitations of biochar-assisted AD processes. Furthermore, the application of electric fields to AD contributes to shorten the lengthy retention time, and it was a major issue in the co-digestion of food and sewage sludge (Sun *et al.* 2020; Liang *et al.* 2021). The addition of food waste to sewage sludge could prevent the exogenous excretion of acidogenic bacteria and the hydrolytic enzyme to enhance the biochemical degradability of substrates in AD (Feng *et al.* 2009; Dai *et al.* 2013; Johnravindar *et al.* 2022). Thus, the co-digestion of food waste and sewage sludge may achieve the same or better effects than the mono-digestion of sewage sludge by applying lower-magnitude electric fields. In this study, we developed a novel approach by coupling a low-magnitude electric field with biogas residue biochar to overcome the incomplete enhancement of gas production and lengthy retention time in biochar-assisted AD. Three different external voltages (0.3, 0.6, and 0.9 V) were applied to investigate the coupled effects on AD where methanogenic properties and process stability in the co-digestion of food waste and sewage sludge were investigated. Furthermore, this study investigated the diversity of microbial communities to elucidate the synergistic mechanisms of the electric fields coupled with biochar in terms of enhancing AD performance and reducing greenhouse gas emissions, together with the potential of this approach for practical applications.

2. MATERIALS AND METHODS

2.1. Substrates and inoculum

The degreased food waste was taken from a food waste plant in Suzhou, China, and the sewage sludge was taken from the secondary settling tank of a wastewater treatment plant in Suzhou. The inoculum was collected from an anaerobic fermenter in the treatment plant. The substrates were taken to the laboratory and stored at 4 °C for later use. The raw material was a mixture of food waste and sewage sludge, combined in a volume ratio of 1:1. Table 1 lists the characteristics of inoculum and raw materials.

2.2. Preparation and characterization of biochar

Biogas residue biochar was prepared and characterized from the biogas residue of AD in our previous study (Liu *et al.* 2022b), and we used the same batch of prepared biochar in this study. The specific properties and analysis of biochar can be found in Supplementary Table S1.

2.3. Experimental design

In this study, the experiments were performed at a temperature of 55 ± 1 °C using four 500 mL bottle anaerobic reactors (300 mL effective volume). These reactors were placed in a shaker with a temperature of 55 ± 1 °C and a speed of 100 rpm, with the experiment lasted for 30 days. The experiment was not domesticated in order to better reflect the effect of low-magnitude electric fields coupled with biochar on AD. 280 mL of the inoculum was prefilled into the bottle reactor and then bubbled with nitrogen for 5 min to ensure an anaerobic condition. 20 mL of feed and 20 mL of discharge were used to measure the biogas production every day, and the fermentation broth and biogas composition were analyzed every 3 days, with all samples taken in triplicate. The pH was stabilized at 7.2–8.2 by the internal adjustment of the system.

The experiment includes four parallel group runs to investigate the effect of the coupling approach on AD (Supplementary Figure S1): (a) the coupled group with the direct voltage and 5 g/L biochar application, (b) the direct voltage group with solely electric field application, (c) the biochar group with solely 5 g/L biochar application, and (d) the control group without biochar and electric field application, where the electric field in groups (c) and (d) was added by inserting a pair of carbon felt electrodes (4 × 4 × 0.5 cm) into the anaerobic reactor. The electrodes were connected to a direct current-regulated power supply through a titanium wire. The carbon fiber electrodes were pretreated before use. This involved soaking them in

Table 1 | Characteristics of digested substrates and inoculum

Parameters	Unit	Sewage sludge	Food waste (FW)	Inoculum	Sewage sludge – FW mixture (1/1, v/v)
pH	/	6.88 ± 0.01	4.23 ± 0.01	7.79 ± 0.01	5.78 ± 0.01
TS	%wt	3.27 ± 0.03	8.08 ± 0.03	4.54 ± 0.03	26.78 ± 0.03
VS	%wt	2.19 ± 0.02	7.04 ± 0.02	3.41 ± 0.02	4.96 ± 0.02
VS/TS	%wt	66.97 ± 0.15	87.12 ± 0.12	75.11 ± 0.18	73.16 ± 0.11
C/N	/	5.86 ± 0.05	11.08 ± 0.04	14.31 ± 0.02	9.22 ± 0.03

1 mol/L hydrochloric acid, followed by washing and drying. The electric field was supplied in three stages, such as 0–10, 11–20, and 21–30 days, and connected to a stabilized voltage of 0.3, 0.6, and 0.9 V, respectively. Previous experiments have shown that 5 g/L is the optimal dosage of the biogas residue biochar (relevant data could be available in Supplementary Figure S2).

2.4. Analytical methods

The gas sampling bag was connected to the gas outlet, and the daily biogas production was measured in the gas sampling bag using a graduated 500 mL gas-tight syringe (Tongji 5 × 4U5, Ningbo, China). Methane production was calculated by multiplying the biogas production by the methane content. The methanogenic capacity was then converted based on the volatile solids content of the daily feedstock.

Biogas was analyzed using a GC9800 gas chromatograph that was equipped with a thermal conductivity detector, and the column used was packed with TDX-01 (2 m × 3 mm). The carrier gas was argon at a pressure of 0.4 MPa, and the peaks of gas chromatography were H_2, N_2, CH_4, and CO_2.

The measurement methods of total solids (TS), volatile solids (VS), total chemical oxygen demand (TCOD), and total nitrogen (TN) were the same as the descriptions in the previous study (Liu *et al.* 2021). The C/N ratio was calculated on the TCOD and TN measured. Measurements of soluble chemical oxygen demand (SCOD) and total ammonia nitrogen (TAN) were made by centrifuging the digested solution collected from the reactor at 4,000 rpm for 10 min, and the extracted supernatant was immediately stored in a refrigerator at 4 °C. Samples were taken within 24 h and filtered through an organic filtration column (0.45 mm) for analytical determination. The filtrate was digested with the potassium dichromate reagent at 150 °C for 2 h to measure the SCOD and then tested for colorimetry on a DR2800 spectrophotometer (HACH Co., Loveland, CO, USA). The concentration of ammonia nitrogen was determined by using Nessler's reagent and the spectrophotometer (Jingke 721G, Shanghai, China) at a wavelength of 420 nm. pH of the digestate was measured by a pH meter (Leici PHBJ-260, Shanghai, China).

A three-dimensional fluorescence spectrometer (F-7000FL, Hitachi, Japan) was used to analyze dissolved organic matter (DOM) in the digested sludge supernatant after passing through a 0.45 μm filter membrane. The fluorescence spectrometer was monitored, and signals were recorded using FL Solutions 4.2 software. The excitation light source was a 150 W xenon lamp. The photomultiplier tube voltage was 700 V. The excitation wavelength (λ-Ex) ranged from 200 to 600 nm in 10 nm steps. The emission wavelength (λ-Em) ranged from 200 to 600 nm in 10 nm steps. The scanning speed was about 12,000 nm/min. To calibrate the instrumental conditions and the effect of Raman scattering on the fluorescence spectra, the ultrapure water (18.25 MΩ-cm) was used as blank (all samples were diluted by a factor of 500 in order to ensure that they were within the measurement range).

The polymerase chain reaction (PCR) and sequencing were carried out according to Xu *et al.* (2017). Microbial communities in sludge collected from the digester at a relatively stable stage were analyzed by high-throughput sequencing. Sludge samples (~1.0 g) from each vial were collected and stored at −20 °C and then these samples were sent to Majorbio (Shanghai, China) for PCR amplification. For pyrophosphate sequencing, archaeal primers 524F10extF (5′-TGYCAGCCGCCGCGGTAA-3′) and Arch958RmodR (5′-YCCGGCGTTGAVTCCAATT-3′) were used to extend the V4–V5 region of the 16S rRNA gene by the PCR. Sequences obtained from the individual samples were then classified into phylum and genus levels, which were then analyzed by pyrophosphate sequencing on the Illumina platform (Illumina Miseq PE300).

3. RESULTS AND DISCUSSION

3.1. Enhanced performances by biochar coupled with low-magnitude electric fields

3.1.1. Enhanced methane yield and accelerated initiation from biochar

Figure 1 shows biogas production (a) and methanogenic capacity (b) in the first 10 days for the four groups. The coupled group (0.3 V/Biochar) had the highest average daily biogas production at 534 mL, surpassing the control (220.0 mL) and biochar (387.2 mL) groups by 143.0 and 37.9%, respectively. Methane yield mirrored this trend (Figure 1(b)), with optimized methanogenic capacity in the coupled group (311.7 mL/g·VS·d), which was 45.5% higher than that of the biochar group (214.2 mL/g·VS·d).

Biochar application alone showed an excellent performance in improving the methane yield. The porous and fragmented structure of residue biochar promoted the growth of specific methanogens via the immobilization effect of biochar, and more

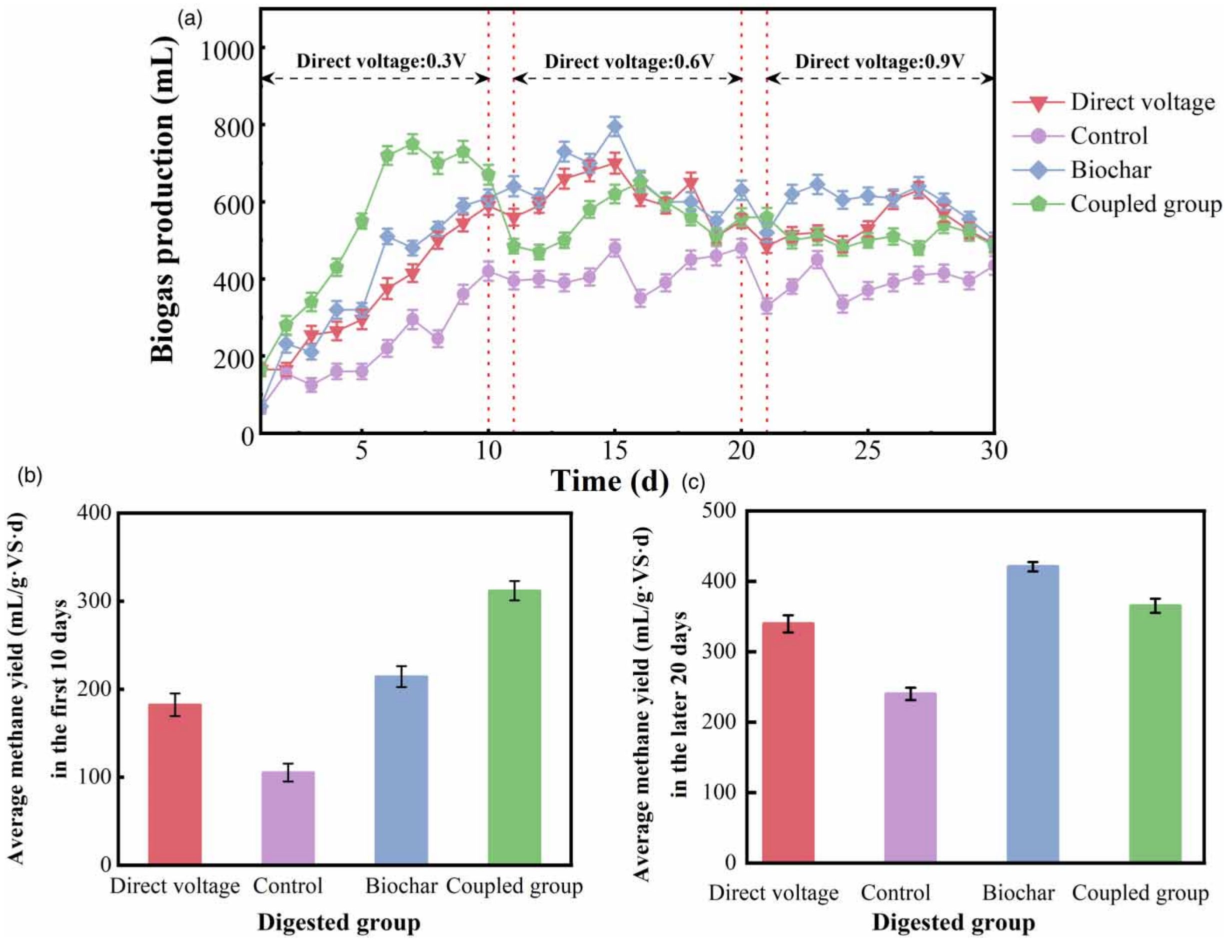

Figure 1 | Biogas production (a), methanogenic properties in the first 10 days (b), and methanogenic properties in the later 20 days (c) for the direct voltage group, control group, biochar group, and coupled group (direct voltage/biochar). Direct voltages added were 0.3 V for the first 10 days, 0.6 V for the next 10 days, and 0.9 V for the last 10 days.

multifunctional groups and basic groups (–OH, CO_3^{2-}, C ≡ C, –NH, C = O) on the surface of biochar would contribute to neutralize fatty acids more effectively. Furthermore, the prepared biochar might promote the DIET process between *Methanobacterium* and *Clostridia* (Liu *et al.* 2022b), which are responsible for improved biogas production. In the first 10 days, the average methane yield of the direct voltage group (0.3 V applied) was 72.9% higher than the control group (Figure 1(b)). The increased methane yield may be due to the action of acetolactic methanogens when the voltage application was below 0.6 V (Sun *et al.* 2020). A low-magnitude electric field increased the strength of sludge flocs by promoting the secretion of extracellular polymeric substances and improving the efficiency of interspecies electron transfer between specific microorganisms, thereby improving methane yield (Gao *et al.* 2017). Therefore, the synergy between biochar and an external voltage of 0.3 V might further improve the efficiency of interspecies electron transfer between microorganisms, which could be critical in optimizing AD start-up and maximizing biogas performance.

The addition of food waste to sewage sludge could prevent the exogenous excretion of acidogenic bacteria and the hydrolytic enzyme, which was beneficial to enhancing the hydrolysis of sewage sludge (Feng *et al.* 2009). The addition of sewage sludge into food waste could dilute toxic substances (salts, heavy metals, ammonia, and volatile fatty acids (VFAs)) and introduce nutrient elements (trace metals) to improve the buffering capacity of AD (Montecchio *et al.* 2019). Thus, the mixture of food waste and sewage sludge enhanced the biochemical degradability of substrates in the system. Based on the above considerations, we chose 0.3 V as the starting voltage and applied 0.6 and 0.9 V voltages in the subsequent second stage (11–20 days) and the third stage (21–30 days).

3.1.2. Methanogenic properties from biochar coupled with 0.6 and 0.9 V

The coupled group in the later 20 days showed a significant decrease compared to the biochar group and the direct voltage group (Figure 1). It was found that the biochar group demonstrated optimal methane production during these stages. The methanogenic property of the direct voltage group in the last 20 days was 41.4% higher than the control group, showing the enhancement of methanogenic capacity. However, the electric field showed a decrease compared to the previous 10 days. It may be attributed to that excessive weak stimulation could cause an increase in surface hydrophobicity, the flattening of cells, and the presence of exudate on the cell surface, stimulating the attachment of bacteria to solid surfaces and thus inhibiting the metabolism of microorganisms (Luo *et al.* 2005). Previous studies also showed that the increased hydrophobicity of microbial surfaces may result in increased microbial mortality when an excessive voltage was applied (Sheng *et al.* 2010). The high conductivity and unique structure of biogas residue biochar may enhance the stimulation effect of excessive voltages and thus limit the enhancement of methanogenic bacterial activity compared to adding biochar alone.

Thus, it could be concluded from this work that an external voltage of 0.3 V coupled with 5 g/L biochar in the first 10 days was more advantageous than 0.6 and 0.9 V. Coupling 5 g/L biochar with the applied electric field could maximize the activation and enrichment of the methanogenic bacteria and minimize the energy input. Furthermore, biochar could improve the performance of AD more efficiently than the low-magnitude electric field. The unique properties of biochar in enriching the microbial community and enhancing the buffering capacity of the system in various aspects may contribute to its better performance.

3.1.3. Improved biogas quality

Figure 2 shows the methane content in biogas for four groups. It demonstrates that the methane content of the coupled group was always higher than that of other groups, indicating that the coupled solution could improve the quality of biogas. The coupled group and the biochar group enhanced biogas quality by 17.7 and 14.7%, respectively. Physical adsorption and carbonation reaction with CO_2 of the biochar may contribute to the improved methane content in the biochar-amended AD. The porous structure of biochar provides a large surface area, allowing it to retain CO_2 and H_2S, while the CH_4 could flow through it due to varied molecular characteristics (Shen *et al.* 2015). High concentrations of monovalent and divalent cations

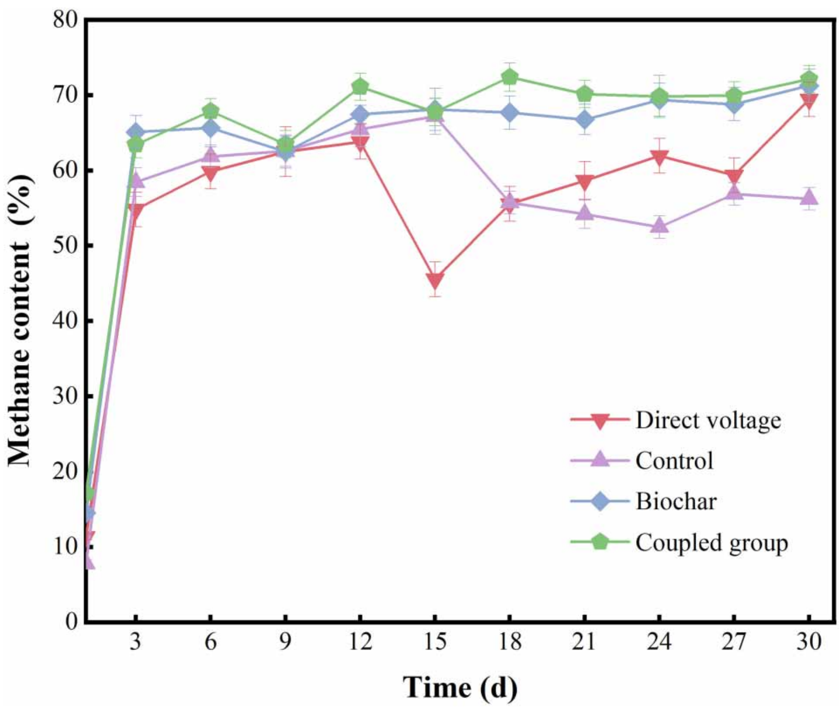

Figure 2 | The methane content in biogas during the 30 days for the direct voltage group, control group, biochar group, and coupled group (direct voltage/biochar).

in biochar could accelerate carbonation reactions with CO_2 (Ahmad *et al.* 2014). Furthermore, biochar may enhance the syntrophic cooperation of organic acid-oxidizing bacteria and CO_2-reducing methanogen by promoting DIET effects (Shen *et al.* 2015). Therefore, the electric field coupled with biochar may enhance the carbonation reaction characteristics of the biogas residue biochar and bring about diverse affinity to biochar compared to adding biochar alone, resulting in a further increase of 3.0% in methane content.

The above results demonstrate that a low-magnitude electric field coupled with biochar contributed to AD initiation, while the excessive voltages coupled with biochar at the maturation stage of methanogenic bacteria did elevate methane content but was not effective in improving methanogenic properties than adding biochar alone.

3.2. Effects of biochar coupled with the low-magnitude electric field on substrate decomposition

3.2.1. Evolutions of pH throughout the cycle

Figure 3(a) shows the evolution of pH in the four digested groups. The pH values of the four groups were between 6.5 and 8.5, which were within an appropriate range for methanogenesis (Vijin Prabhu *et al.* 2021). The pH of the control group decreased during the first 3 days of the reaction due to the accelerated rate of hydrolysis and rapid acidification of the substrates under the thermophilic conditions (55 ± 1 °C), while the pH values of both the biochar group and the coupled group

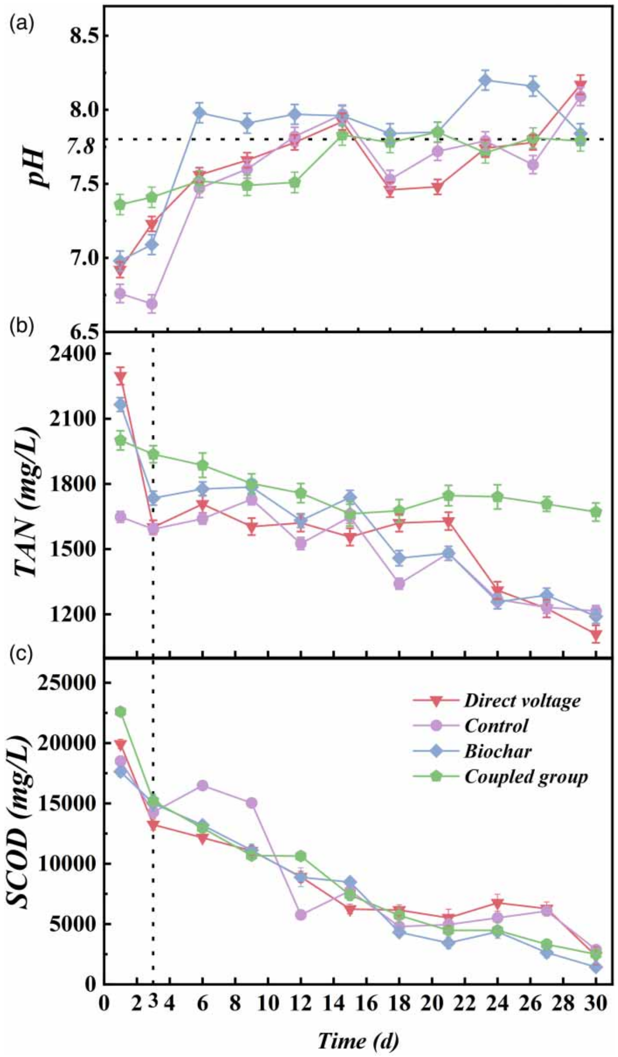

Figure 3 | Evolution of pH (a), TAN (b), and SCOD (c) in the anaerobic co-digestion of food waste and sewage sludge over the 30 days for the direct voltage group, control group, biochar group, and coupled group (direct voltage/biochar).

in the first 3 days were higher than those of the control group. Biochar has a higher buffering capacity for pH under thermophilic conditions than mesophilic conditions, reducing the detrimental effect of VFA and enhancing the system stability (Guo *et al.* 2014), and more alkaline functional groups on the surface of residue biochar could neutralize the VFAs more effectively (Liu *et al.* 2022b). Thus, the higher and more stable pH of the biochar group (~8.0) exacerbated the consumption of VFA, resulting in excellent methanogenic capacity in the whole reaction.

The initial pH of the direct voltage group was higher than that of the control group and did not decrease, demonstrating that the applied electric field also alleviated the acid inhibition and reduced the lag period of methanogenesis. Meanwhile, adding an electric field was not as effective as adding biochar in initiating AD, which could be attributed to the multifaceted role of biochar in enriching microflora and enhancing the buffering capacity of the system.

The pH of the coupled group in the initial stage (the first 10 days) was more stable than the other groups, again confirming that the synergistic effect of biochar and low-magnitude electric fields helped to better mitigate the acidification effect and promote the activation of methanogenic bacteria. However, the pH of the coupled group was significantly lower than that of the biochar group over the following 20 days, indicating that the coupling of excessive low-magnitude electric fields and biochar reduced the efficiency of utilizing VFAs, which could be attributed to the limited improvement in methanogenic activity. Thus, the coupling of appropriate magnitude electric fields and biochar could enhance substrate utilization efficiency and hence yield methanogenic capacity in AD.

3.2.2. Evolutions of TAN throughout the cycle

Figure 3(b) shows the evolution of ammonia nitrogen concentration in the four digested groups over 30 days. Although ammonia nitrogen could provide essential nutrients to anaerobic microorganisms and provide partial alkalinity to the system, excessive nitrogen could affect the stability (Yuan & Zhu 2016).

Ammonia concentrations in the four groups decreased from 2,400 to 1,100 mg/L. The ammonia nitrogen levels of the other three groups was higher than those in the control group during the first 3 days and decreased rapidly. This may be that the accelerated hydrolysis of the substrate by the biochar, the low-magnitude electric field, and the coupling of the two aspects promoted the release and disintegration of more organic nitrogen (proteins, urea, amino, nucleic, or uric acid). The ammonia nitrogen decreased slowly after 3 days, probably due to the continuous absorption and utilization by anaerobic bacteria. The semi-continuous flow reduced the inhibition effect of intermediates on the anaerobic reaction through the exchange of materials, avoiding the accumulation of ammonia nitrogen. Some studies showed that the level of ammonia nitrogen in the experimental group with biochar added was lower than that of the control group due to the adsorption by biochar (Mumme *et al.* 2014; Zhang *et al.* 2023). However, the opposite trend was observed in the biochar group and the coupled group with biochar added in this study. This may be because biogas residue biochar has a greater effect on the hydrolysis efficiency of the substrate than on the adsorption of ammonia nitrogen, and it could also reflect the semi-continuous flow mode of operation as opposed to the continuous flow. The more stable level of ammonia nitrogen in the coupled group during the following 20 days suggested that the couplings of the excessive electric fields and the biochar limited the increase in hydrolysis efficiency of the substrate, resulting in a decrease in biogas production in the later stage compared to that over the first 10 days. Thus, appropriate magnitude electric fields coupled with biochar could maximize the utilization efficiency of substrates and methanogenic capacity.

3.2.3. Evolutions of SCOD and DOM

The evolution of SCOD in different digesters is demonstrated in Figure 3(c). SCOD reflects the degree of substrate hydrolysis and the utilization of organic compounds (e.g., VFA, soluble proteins, and soluble polysaccharides) in the current reactor (Chen *et al.* 2016). During the first 3 days, the concentration of SCOD decreased significantly in all groups, with the fastest decrease in the coupled group, indicating that both the biochar and electric field helped to accelerate the hydrolysis and increase the consumption rate of soluble organic matter in the early stage. Thus, the coupling of biochar and low-magnitude electric fields further enhanced the rate of the degradation of organic matter, improving the methanogenic properties significantly during the first 10 days. The lower concentration of SCOD in the biochar group in the stage was closely correlated with the higher pH (Figure 3(a)), and this could be attributed to the enhanced VFA conversion by biochar, suggesting that biochar could reduce the accumulation of intermediates and accelerate their utilization. Meanwhile, the levels of SCOD in the remaining three groups were lower than that of the control group, also confirming the positive effect of biochar addition on organic matter conversion and methanation. Thus, biochar and coupled effect provided more stable and efficient degradation than electric fields in the first 10 days, while the coupled effect demonstrated superior methanogenic properties in the stage. Furthermore, the concentration of SCOD in the coupled group was lower than that in the biochar group in the later stages (11–30 days), while the biochar group showed better biogas production performance than the coupled effect in this stage, again indicating that the excessive electric fields coupled with biochar limited the improvement in the efficiency of hydrolyzing and utilizing organic matter.

The evolution of DOM was observed in the four digested reactors, with changes in migration on days 5, 15, and 30 (Supplementary Figure S3). The fluorescence peaks in the protein-like region (Ex/Em = 280/300–350 nm) and the lignocellulose region (Ex/Em = 220/300–350 nm) of the biochar group and the coupled group were more pronounced than those of the control group on day 5, indicating that the addition of biochar promoted the precipitation of proteins and cellulose to provide more nutrients for microorganisms, thereby improving biogas production performance. However, the opposite change occurred in the direct voltage group. The applied electric fields have been proven to enhance organics removal and methane yield by boosting electron transfer efficiency and activate microorganisms (Mendoza-Tinoco *et al.* 2023). Thus, the change might be attributed to that the applied electric field had already accelerated the utilization of DOM by microorganisms during the first 5 days. Moreover, the fluorescence intensity of the coupled group was weaker than that of the biochar group, while it demonstrated the optimal methanogenic property during the first 10 days. Granular activated carbon (GAC) could be polarized by an external electric field, creating a reducing/oxidizing microenvironment and promoting organic matter degradation (Sun *et al.* 2022). Thus, the polarization of biochar by the electric field may accelerate the decomposition and utilization of organics, and ultimately, the coupled group showed superior methanogenic properties over the first 10 days. However, the fluorescence intensity of the coupled group was higher than that of the biochar group on days 15 and 30. This demonstrated that excessive electric fields coupled with biochar may limit the enhancement of microbial activity and reduce the efficiency of organic matter utilization, resulting in inferior biogas production performance to that of biochar over the subsequent 20 days. Thus, the coupling of appropriate magnitude electric fields and biochar could optimize the efficiency of utilizing substrates and maximize methanogenic capacity.

3.3. Functional microbial community stimulated by the coupled approach

Figure 4 reveals the distribution of archaeal communities in four groups of reactors after 10 days. The coupling method provided optimal methanogenic capacity during the first 10 days, so the microbial community constituents of AD were analyzed by high-throughput sequencing to evaluate the reasons for the coupling effect on enhancing biogas production performance.

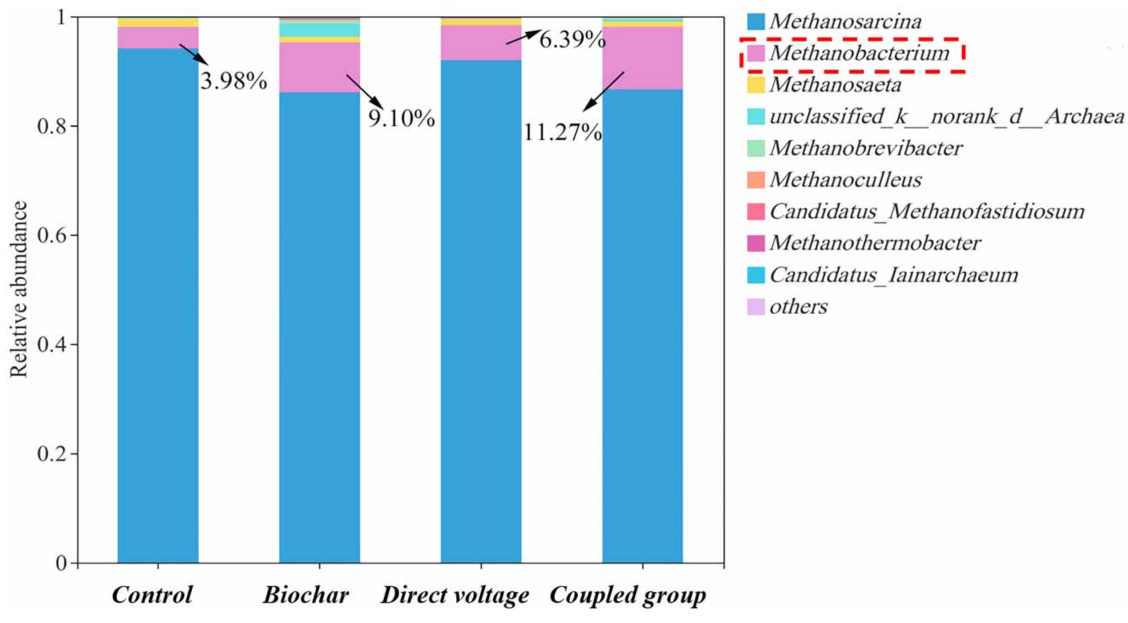

Figure 4 | Bar graph of archaeal communities for the direct voltage group, control group, biochar group, and coupled group (direct voltage/biochar).

Our previous work found that several types of biochar including biogas residue biochar had similar effects on bacterial communities and greater effects on archaeal communities during the co-digestion of sewage sludge and food waste (Liu *et al.* 2022b). Thus, we focused on the coupled effect on archaeal communities in this work.

Primary methanogens observed in the four groups included *Methanobacterium*, *Methanosarcina*, and *Methanosaeta*. *Methanosarcina* are polymorphic methanogens, capable of producing methane from H_2 and acetate as well as methane from CO_2 by DIET reduction (Rotaru *et al.* 2014). *Methanosaeta*, known as acetate-consuming methanogens, can directly accept electrons from conductive materials (Gonzalez-Fernandez *et al.* 2015; Lei *et al.* 2018). Thus, *Methanosarcina* and *Methanosaeta* may play a significant role in the methanogenesis stage and establish DIET with electroactive bacteria for methane production. However, the relative abundance of these two methanogens was higher in the control group than in the other groups, which was contrary to the analysis of biogas production properties, again indicating that other microorganisms such as *Methanobacterium* may play a more significant role in enhancing methanogenic performance.

The relative abundance of *Methanobacterium* in each group was 3.98% (control group), 6.4% (direct voltage group), 9.1% (biochar group), and 11.3% (coupled group), and this magnitude trend was consistent with the methanogenic performance in this stage. *Methanobacterium*, recognized as hydrogen-consuming methanogens, could produce CH_4 through hydrogenotrophic methanogenesis from H_2 and CO_2, as well as accept electrons to form CH_4 directly (Morita *et al.* 2011; Lin *et al.* 2018). It has exhibited a higher relative abundance in the direct voltage group and the biochar group than in the control group. Low-magnitude electric fields allow the extraction of carbohydrates, lipids, and proteins, among other biomolecules, without losing cellular integrity (Eing *et al.* 2013), and it could selectively enrich specific methanogens and reduce the abundance of other methanogens to modulate the methanogenic pathway (Jiang *et al.* 2022). Thus, it could be found that the separate action of the external voltage of 0.3 V increased the abundance of *Methanobacterium* from 4.0 to 6.4% and decreased the relative abundance of *Methanosarcina* from 94.2 to 92.0% in this study. Meanwhile, the archaeal were enriched in the biochar group and the relative abundance of *unclassified_k_norank_d_Archaea* was the highest of the four experimental groups, even exceeding the coupled group. This enhancement may be attributed to the eco-compatibility and porous structures of biochar, offering a refuge for microbial adhesion (Chen *et al.* 2021). The thermophilic hydrogen-consuming methanogens, *Methanothermobacter* and *Methanobrevibacter*, were also identified in addition to the increased *Methanobacterium*, with optimal metabolic temperatures between 55 and 65 °C (Lin *et al.* 2018). Thus, the low-magnitude electric field coupled with biochar increased the species richness and selectively enriched specific methanogens such as *Methanosarcina* and *Methanobacterium* to modulate the methanogenic pathway in this work.

Furthermore, the applied electric field could increase the number of electroactive bacteria simultaneously, such as *Geobacter* species, which facilitates long-range electron transfer through conductive pili and improves the DIET efficiency to enhance methane production (Ambuchi *et al.* 2017; Sun *et al.* 2020). Biogas residue biochar could also promote the growth of DIET-mediated electroactive bacteria, such as *Clostridia* (Liu *et al.* 2022b). Thus, coupling biochar with an electric field allows for the better enrichment of specific methanogens and bacteria and enhances the DIET mechanism between them, enhancing methanogenic performances ultimately.

3.4. Proposed pathways by the coupled approach in AD

Figure 5 illustrates the potential mechanisms of biochar coupled with a low-magnitude electric field in enhancing methane yield within the initial 10 days. The presence of functional groups, such as aromatic and carbonyl groups, on the surface of biogas residue biochar greatly enhances its electron transfer capacity (Qi *et al.* 2021; Liu *et al.* 2022b; Jin *et al.* 2023). Coupling biochar with moderate magnitude electric fields further enhances electron transfer efficiency in AD. Moreover, the coupled approach enriches specific bacteria and hydrogen-consuming methanogens like *Methanobacterium* and *Methanosarcina*, which can also participate in DIET, and reduces acetolactic methanogenesis such as *Methanosaeta*. Thus, the coupled approach promotes methane production by weakening acetolactic methanogenesis and strengthening hydrogenotrophic methanogenesis and the DIET mechanism associated with electroactive bacteria.

3.5. Implications of the coupled approach in AD

The coupling of biochar and low-magnitude electric fields was used to enhance the performance of biochar-assisted AD and mitigate prolonged retention time in the co-digestion of food waste and sewage sludge. Results revealed that the integration of biogas residue biochar with a moderate magnitude electric field promoted the initiation of AD. Additionally, the coupled approach involving an external voltage of 0.3 V demonstrated a moderate enhancement in methane production throughout

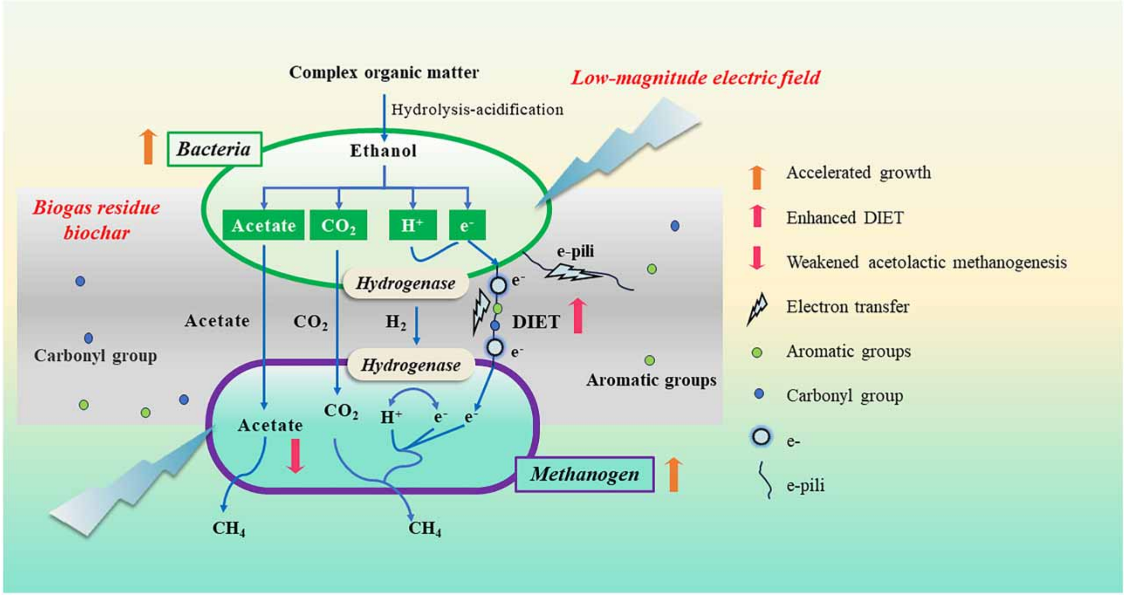

Figure 5 | Potential mechanisms of biogas residue biochar coupled with low-magnitude electric fields on methane production enhancement from AD.

the cycle when compared to the sole addition of biochar. Previous work focused on incorporating iron species into carbon-based material to enhance the performance of AD with biochar-assisted, which could enhance the efficiency of electron transfer in the AD system and supply more adsorption sites for iron oxide (Sun *et al.* 2021; Chen *et al.* 2022; Liu *et al.* 2022a; Jin *et al.* 2023). However, the effectiveness of the composite for AD of actual substrates remains to be investigated because the synthetic substrates were used in these studies, and the cost of synthesizing the composite materials (impregnation and co-precipitation) is more expensive and cumbersome than ball-milling/carbonization (Sun *et al.* 2021; Chen *et al.* 2022). On the other hand, although the magnetic biochar was applied to enhance AD of waste-activated sludge (Jin *et al.* 2023), the biochar improved methane production by 22.1%, where the enhancement effect was not as effective as in this study (45.5%) and its production costs are higher. Magnetic biochar, which is prepared through the process of ball-milling/carbonization, has also been found to enhance AD efficiencyy (Liu *et al.* 2022a), while the cost of purchasing and transporting raw materials needs to be considered in practical applications and its preparation process was more cumbersome than the coupled approach in the study. Moreover, the GAC loaded with nanoscale zero-valent iron (NZVI) coupled with direct voltage was also applied to enhance AD of synthetic wastewater (Sun *et al.* 2022), while the reaction time was very short and the methane yield was boosted only 10.83% within 12 h. These findings demonstrate the feasibility and better application prospects of electric fields coupled with biochar, where on-site recycling of biogas residue combined with small energy inputs could realize multiple benefits, such as lower by-product disposal costs, higher gas production efficiency, and lower operating costs. Furthermore, the commercial value of biogas residue biochar could be considered for development, given its superior performance over other biochar in enhancing methane production in AD due to its unique characteristics (Liu *et al.* 2022b).

Future studies may conduct detailed energy consumption analysis (electrical energy inputs and costs to prepare the biochar) and analyze the benefits generated, such as gains in biogas production and savings in biogas purification as well as reductions in the cost of biogas residue disposal. Furthermore, biochar can serve as electrode materials in voltage-enhanced AD reactors (carbon fiber electrodes were used in this study), offering a novel solution for its recycling from reactors. Subsequent investigations could explore the effect of biochar coupled with electric fields on the hydrolysis-acidification of substrates by analyzing the key intermediate metabolites for methanogenesis such as VFAs and soluble proteins. Additionally, hydrogenase, which could catalyze the production of H_2 produced by fermentation bacteria during the interspecies hydrogen transfer process (Guss Adam *et al.* 2009), and CoF420 as indicators of methanogenic activity (Xu *et al.* 2018), combined with comprehensive microbial community analysis, would provide insights into the detailed mechanism of biochar coupled with electric fields to enhance AD.

4. CONCLUSIONS

The effect of coupling biochar with low-magnitude electric fields on the performance of AD was investigated. The findings demonstrated that coupling of an external voltage of 0.3 V coupled with 5 g/L of biochar resulted in a 143% surge in biogas production. Moreover, during the initial phase of the reaction, the coupled approach substantially elevated CH_4 yield by 45.5 and 71.0% in comparison to biochar alone and the sole application of direct voltage, respectively. This coupled approach increased methane production by enriching hydrogenotrophic methanogens such as *Methanobacterium*, enhancing DIET associated with electroactive bacteria and weakening acetolactate methanogenic capacity. The coupled approach also enhanced biogas quality, expedited the efficient utilization of VFA, and accelerated ammonia nitrogen removal in the early stages, thereby improving the start-up efficiency of AD. On-site recovery of biochar derived from biogas residues, coupled with low-magnitude electric fields, provides a novel strategy to enhance methanogenic performance, improve biogas quality, and maximize resource utilization of by-products in AD. Furthermore, the coupled approach exhibits superior application potential to enhance the performance with biochar assistance when compared to alternative methods, such as the incorporation of iron species into biochar. These findings underscore the synergistic capabilities of biochar and low-magnitude electric fields in advancing the performance of AD, offering valuable insights for its broader application.

ACKNOWLEDGEMENTS

The authors would like to acknowledge the co-funding of this work by Projects of International Cooperation Shanghai (STCSM, 23230711300), the National Natural Science Foundation of China (No. 52070130), and the Science and Technology Planning Project of Taizhou City, Jiangsu Province.

DATA AVAILABILITY STATEMENT

All relevant data are included in the paper or its Supplementary Information.

CONFLICT OF INTEREST

The authors declare there is no conflict.

REFERENCES

Ahmad, M., Rajapaksha, A. U., Lim, J. E., Zhang, M., Bolan, N., Mohan, D., Vithanage, M., Lee, S. S. & Ok, Y. S. 2014 Biochar as a sorbent for contaminant management in soil and water: A review. *Chemosphere* **99**, 19–33.

Ambuchi, J. J., Zhang, Z., Shan, L., Liang, D., Zhang, P. & Feng, Y. 2017 Response of anaerobic granular sludge to iron oxide nanoparticles and multi-wall carbon nanotubes during beet sugar industrial wastewater treatment. *Water Research* **117**, 87–94.

Chen, Y., Yu, B., Yin, C., Zhang, C., Dai, X., Yuan, H. & Zhu, N. 2016 Biostimulation by direct voltage to enhance anaerobic digestion of waste activated sludge. *RSC Advances* **6** (2), 1581–1588.

Chen, M., Liu, S., Yuan, X., Li, Q. X., Wang, F., Xin, F. & Wen, B. 2021 Methane production and characteristics of the microbial community in the co-digestion of potato pulp waste and dairy manure amended with biochar. *Renewable Energy* **163**, 357–367.

Chen, J., Zhang, P., Zhang, J., He, Y. & Tong, Y. W. 2022 Micro–nano magnetite-loaded biochar enhances interspecies electron transfer and viability of functional microorganisms in anaerobic digestion. *ACS Sustainable Chemistry & Engineering* **10** (8), 2811–2821.

Dai, X., Duan, N., Dong, B. & Dai, L. 2013 High-solids anaerobic co-digestion of sewage sludge and food waste in comparison with mono digestions: Stability and performance. *Waste Management* **33** (2), 308–316.

Eing, C., Goettel, M., Straessner, R., Gusbeth, C. & Frey, W. 2013 Pulsed electric field treatment of microalgae – benefits for microalgae biomass processing. *IEEE Transactions on Plasma Science* **41** (10), 2901–2907.

Feng, L., Chen, Y. & Zheng, X. 2009 Enhancement of waste activated sludge protein conversion and volatile fatty acids accumulation during waste activated sludge anaerobic fermentation by carbohydrate substrate addition: The effect of pH. *Environmental Science & Technology* **43** (12), 4373–4380.

Fuchs, W. & Drosg, B. 2013 Assessment of the state of the art of technologies for the processing of digestate residue from anaerobic digesters. *Water Science and Technology* **67** (9), 1984–1993.

Gao, Y., Sun, D., Dang, Y., Lei, Y., Ji, J., Lv, T., Bian, R., Xiao, Z., Yan, L. & Holmes, D. E. 2017 Enhancing biomethanogenic treatment of fresh incineration leachate using single chambered microbial electrolysis cells. *Bioresource Technology* **231**, 129–137.

Gonzalez-Fernandez, C., Sialve, B. & Molinuevo-Salces, B. 2015 Anaerobic digestion of microalgal biomass: Challenges, opportunities and research needs. *Bioresource Technology* **198**, 896–906.

Guo, X., Wang, C., Sun, F., Zhu, W. & Wu, W. 2014 A comparison of microbial characteristics between the thermophilic and mesophilic anaerobic digesters exposed to elevated food waste loadings. *Bioresource Technology* **152**, 420–428.

Guss Adam, M., Kulkarni, G. & Metcalf William, W. 2009 Differences in hydrogenase gene expression between *Methanosarcina acetivorans* and *Methanosarcina barkeri*. *Journal of Bacteriology* **191** (8), 2826–2833.

Hao, X., Batstone, D. & Guest, J. S. 2015 Carbon neutrality: An ultimate goal towards sustainable wastewater treatment plants. *Water Research* **87**, 413–415.

Hoang, A. T., Goldfarb, J. L., Foley, A. M., Lichtfouse, E., Kumar, M., Xiao, L., Ahmed, S. F., Said, Z., Luque, R., Bui, V. G. & Nguyen, X. P. 2022 Production of biochar from crop residues and its application for anaerobic digestion. *Bioresource Technology* **363**, 127970.

Jiang, Z., Yu, Q., Sun, C., Wang, Z., Jin, Z., Zhu, Y., Zhao, Z. & Zhang, Y. 2022 Additional electric field alleviates acidity suppression in anaerobic digestion of kitchen wastes via enriching electro-active methanogens in cathodic biofilms. *Water Research* **212**, 118118.

Jin, H. Y., Yang, L., Ren, Y. X., Tang, C. C., Zhou, A. J., Liu, W., Li, Z., Wang, A. & He, Z. W. 2023 Insights into the roles and mechanisms of a green-prepared magnetic biochar in anaerobic digestion of waste activated sludge. *Science of the Total Environment* **896**, 165170.

Johnravindar, D., Kaur, G., Liang, J., Lou, L., Zhao, J., Manu, M. K., Kumar, R., Varjani, S. & Wong, J. W. C. 2022 Impact of total solids content on biochar amended co-digestion of food waste and sludge: Microbial community dynamics, methane production and digestate quality assessment. *Bioresource Technology* **361**, 127682.

Lei, Y., Wei, L., Liu, T., Xiao, Y., Dang, Y., Sun, D. & Holmes, D. E. 2018 Magnetite enhances anaerobic digestion and methanogenesis of fresh leachate from a municipal solid waste incineration plant. *Chemical Engineering Journal* **348**, 992–999.

Liang, J., Luo, L., Li, D., Varjani, S., Xu, Y. & Wong, J. W. C. 2021 Promoting anaerobic co-digestion of sewage sludge and food waste with different types of conductive materials: Performance, stability, and underlying mechanism. *Bioresource Technology* **337**, 125384.

Lin, R., Cheng, J., Ding, L. & Murphy, J. D. 2018 Improved efficiency of anaerobic digestion through direct interspecies electron transfer at mesophilic and thermophilic temperature ranges. *Chemical Engineering Journal* **350**, 681–691.

Liu, H., Wang, X., Qin, S., Lai, W., Yang, X., Xu, S. & Lichtfouse, E. 2021 Comprehensive role of thermal combined ultrasonic pre-treatment in sewage sludge disposal. *Science of the Total Environment* **789**, 147862.

Liu, H., Xu, Y., Li, L., Yuan, S., Geng, H., Tang, Y. & Dai, X. 2022a A novel green composite conductive material enhancing anaerobic digestion of waste activated sludge via improving electron transfer and metabolic activity. *Water Research* **220**, 118687.

Liu, H. B., Wang, X. K., Fang, Y. Y., Lai, W. J., Xu, S. Y. & Lichtfouse, E. 2022b Enhancing thermophilic anaerobic co-digestion of sewage sludge and food waste with biogas residue biochar. *Renewable Energy* **188**, 465–475.

Luo, Q., Wang, H., Zhang, X. & Qian, Y. 2005 Effect of direct electric current on the cell surface properties of phenol-degrading bacteria. *Applied and Environmental Microbiology* **71** (1), 423–427.

Mendoza-Tinoco, T. P., Sanchez-Vazquez, V., Del Carmen Fajardo-Ortiz, M., Gonzalez, I. & Beristain-Cardoso, R. 2023 How does a low-magnitude electric field influence anaerobic digestion in wastewater treatment? A review. *Chemosphere* **325**, 138402.

Montecchio, D., Astals, S., Di Castro, V., Gallipoli, A., Gianico, A., Pagliaccia, P., Piemonte, V., Rossetti, S., Tonanzi, B. & Braguglia, C. M. 2019 Anaerobic co-digestion of food waste and waste activated sludge: ADM1 modelling and microbial analysis to gain insights into the two substrates' synergistic effects. *Waste Management* **97**, 27–37.

Morita, M., Malvankar Nikhil, S., Franks Ashley, E., Summers Zarath, M., Giloteaux, L., Rotaru Amelia, E., Rotaru, C. & Lovley Derek, R. 2011 Potential for direct interspecies electron transfer in methanogenic wastewater digester aggregates. *mBio* **2** (4). doi:10.1128/mbio.00159-11.

Mumme, J., Srocke, F., Heeg, K. & Werner, M. 2014 Use of biochars in anaerobic digestion. *Bioresource Technology* **164**, 189–197.

Park, J. G., Lee, B., Kwon, H. J., Park, H. R. & Jun, H. B. 2019 Effects of a novel auxiliary bio-electrochemical reactor on methane production from highly concentrated food waste in an anaerobic digestion reactor. *Chemosphere* **220**, 403–411.

Qi, Q., Sun, C., Cristhian, C., Zhang, T., Zhang, J., Tian, H., He, Y. & Tong, Y. W. 2021 Enhancement of methanogenic performance by gasification biochar on anaerobic digestion. *Bioresource Technology* **330**, 124993.

Rotaru, A.-E., Shrestha Pravin, M., Liu, F., Markovaite, B., Chen, S., Nevin Kelly, P. & Lovley Derek, R. 2014 Direct interspecies electron transfer between *Geobacter metallireducens* and *Methanosarcina barkeri*. *Applied and Environmental Microbiology* **80** (15), 4599–4605.

Shen, Y., Linville, J. L., Urgun-Demirtas, M., Schoene, R. P. & Snyder, S. W. 2015 Producing pipeline-quality biomethane via anaerobic digestion of sludge amended with corn Stover biochar with in-situ CO_2 removal. *Applied Energy* **158**, 300–309.

Sheng, G.-P., Yu, H.-Q. & Li, X.-Y. 2010 Extracellular polymeric substances (EPS) of microbial aggregates in biological wastewater treatment systems: A review. *Biotechnology Advances* **28** (6), 882–894.

Sun, M., Zhang, Z., Lv, M., Liu, G. & Feng, Y. 2020 Enhancing anaerobic digestion performance of synthetic brewery wastewater with direct voltage. *Bioresource Technology* **315**, 123764.

Sun, M., Zhang, Z., Liu, G., Lv, M. & Feng, Y. 2021 Enhancing methane production of synthetic brewery water with granular activated carbon modified with nanoscale zero-valent iron (NZVI) in anaerobic system. *Science of the Total Environment* **760**, 143933.

Sun, M., Jiang, H., Zhang, Z., Lv, M., Liu, G. & Feng, Y. 2022 Coupling direct voltage and granular activated carbon modified nanoscale zero valent iron for enhancing anaerobic methane production. *Chemosphere* **286** (Pt 3), 131840.

Thakur, H., Verma, N. K., Dhar, A. & Powar, S. 2024 Anaerobic co-digestion of food waste and bio flocculated sewage sludge towards bio-methane production. *Energy Reports* **11**, 2867–2876.

Vijin Prabhu, A., Antony Raja, S., Avinash, A. & Pugazhendhi, A. 2021 Parametric optimization of biogas potential in anaerobic co-digestion of biomass wastes. *Fuel* **288**, 119574.

Wu, C., Zhi, D., Yao, B., Zhou, Y., Yang, Y. & Zhou, Y. 2022 Immobilization of microbes on biochar for water and soil remediation: A review. *Environmental Research* **212**, 113226.

Xu, S., Lu, W., Liu, Y., Ming, Z., Liu, Y., Meng, R. & Wang, H. 2017 Structure and diversity of bacterial communities in two large sanitary landfills in China as revealed by high-throughput sequencing (MiSeq). *Waste Management* **63**, 41–48.

Xu, S., Han, R., Zhang, Y., He, C. & Liu, H. 2018 Differentiated stimulating effects of activated carbon on methanogenic degradation of acetate, propionate and butyrate. *Waste Management* **76**, 394–403.

Xu, C., Bao, Z., Hu, C. & Lyu, L. 2023 Surface electron-polarized biochar-enhanced anaerobic digestion mechanism revealed by metagenomic binning strategy. *Chemical Engineering Journal* **471**, 14474.

Yuan, H. & Zhu, N. 2016 Progress in inhibition mechanisms and process control of intermediates and by-products in sewage sludge anaerobic digestion. *Renewable and Sustainable Energy Reviews* **58**, 429–438.

Zhang, R., Zhang, M., Mou, H., An, Z., Fu, H., Su, X., Chen, C., Chen, J., Lin, H. & Sun, F. 2023a Comparation of mesophilic and thermophilic anaerobic co-digestion of food waste and waste activated sludge driven by biochar derived from kitchen waste. *Journal of Cleaner Production* **408**, 137123.

Zhu, X., Xu, Y., Zhen, G., Lu, X., Xu, S., Zhang, J., Gu, L., Wen, H., Liu, H., Zhang, X. & Wu, Z. 2023 Effective multipurpose sewage sludge and food waste reduction strategies: A focus on recent advances and future perspectives. *Chemosphere* **311** (Pt 1), 136670.

First received 30 January 2024; accepted in revised form 2 April 2024. Available online 12 April 2024